

*Supporting information for*

**Locked-Flavylium Fluorescent Dyes with Tunable  
Emission Wavelengths Based on Intramolecular  
Charge Transfer for Multi-color Ratiometric  
Fluorescence Imaging**

Hua Chen,<sup>‡</sup> Weiyang Lin,<sup>\*,†,‡</sup> Wenqing Jiang,<sup>‡</sup> Baoli Dong,<sup>†</sup> Haijun Cui<sup>‡</sup>,  
and Yonghe Tang<sup>†</sup>

<sup>†</sup> Institute of Fluorescent Probes for Biological Imaging, School of Chemistry and Chemical Engineering, School of Biological Science and Technology, University of Jinan, Jinan, Shandong 250022, P.R. China.

<sup>‡</sup> State Key Laboratory of Chemo/Biosensing and Chemometrics, College of Chemistry and Chemical Engineering, Hunan University, Changsha, Hunan 410082, P. R. China

E-mail: [weiyanglin2013@163.com](mailto:weiyanglin2013@163.com)

## Table of Contents

	Pages
Materials and instruments .....	3
General Procedure for synthesis .....	4
Scheme S1.....	6
Figure S1.....	7
Scheme S2.....	8
Figure S2.....	8
Figure S3.....	8
Figure S4.....	9
Table S1 .....	9
Figure S5.....	10
Figure S6.....	10
Figure S7.....	11
Figure S8.....	11
Figure S9.....	12
Figure S10.....	12
Figure S11.....	13
Figure S12.....	13
Figure S13.....	14
Figure S14.....	14
Figure S15.....	15
Figure S16.....	15
Figure S17.....	16
Figure S18.....	17
Figure S19.....	17
Figure S20.....	18
Figure S21.....	18
Figure S22.....	19
Figure S23.....	19

**Materials and instruments.** Unless otherwise stated, all reagents were purchased from commercial suppliers and used without further purification. Solvents used were purified by standard methods prior to use. Twice-distilled water was used throughout all experiments. High resolution mass spectrometric (HRMS) analyses were measured on a Finnigan MAT 95 XP spectrometer; NMR spectra were recorded on an INOVA-400 spectrometer, using TMS as an internal standard; Electronic absorption spectra were obtained on a LabTech UV Power spectrometer; Photoluminescent spectra were recorded with a HITACHI F4600 fluorescence spectrophotometer with a 1 cm standard quartz cell; The fluorescence imaging of cells was performed with OLYMPUS FV1000 (TY1318) confocal microscopy; The pH measurements were carried out on a Mettler-Toledo Delta 320 pH meter; TLC analysis was performed on silica gel plates and column chromatography was conducted over silica gel (mesh 200–300), both of which were obtained from the Qingdao Ocean Chemicals. Image-Pro® Plus 6.0 program was used for calculation the ratios determination.

**Calculation of pK<sub>a</sub> Values.** pK<sub>a</sub> values of LF dyes at acidic to near-neutral pH regions were calculated by regression analysis of the fluorescence data to fit equation (1)

$$\text{pH} - \text{pK}_a = \log (F_{\text{max}} - F)/(F - F_{\text{min}}) \quad (1)$$

Where F is the area under the corrected emission curve, F<sub>max</sub> and F<sub>min</sub> are maximum and minimum limiting values of F, respectively.

**HeLa cells culture and imaging of pH variations using LF dye.** HeLa cells were cultured in DMEM (Dulbecco's Modified Eagle Medium) supplemented with 10% FBS (fetal bovine serum) in an atmosphere of 5% CO<sub>2</sub> and 95% air at 37 °C. For detection of pH, HeLa cells were incubated with 5.0 μM LF dye for 30 minutes in an atmosphere of 5% CO<sub>2</sub> and 95% air, and then washed with PBS medium of varying pH values (pH 3.5-8.0) containing nigericin (1μg/mL) three times, followed by incubating with the corresponding PBS for another 15 minutes. Subsequently, the cells were imaged using OLYMPUS FV1000 (TY1318) confocal microscope with an

excitation filter of 488 nm.

**Cytotoxicity assays.** HeLa cells were grown in the modified Eagle's medium (MEM) supplemented with 10% FBS (fetal bovine serum) in an atmosphere of 5% CO<sub>2</sub> and 95% air at 37 °C. Immediately before the experiments, the cells were placed in a 96-well plate, followed by addition of increasing concentrations of **LF2-3** and **LF3** (99% MEM and 1% DMSO). The final concentrations of **LF2-3** and **LF3** were 5, 10, 20, 30 μM (n = 5), respectively. The cells were then incubated at 37 °C in an atmosphere of 5% CO<sub>2</sub> and 95% air at 37 °C for 24 h, followed by MTT assays. Untreated assay with MEM (n = 5) was also conducted under the same conditions.

**General Procedure for synthesis of compounds LF.** A mixture of salicylaldehyde derivatives (**1-3**, 0.01 M) and benzocyclohexanone derivatives (**4-6**, 0.01M) in 70% concentrated sulfuric acid 5ml was stirred at 90 °C for 5h at N<sub>2</sub> atmosphere. Subsequently, it was poured onto 100 g of crushed iced and mixed carefully. Perchloric acid (70%, 0.1 ml) was added after stirred 10 min then the aqueous phase is extracted with dichloromethane/MeOH (5 × 100 ml, V/V 10: 1). Especially, **LF3**, in light of its good water solubility, it was poured onto 60 g of crushed iced and mixed carefully. Perchloric acid (70%, 0.1 ml) was added after stirred for 10 min then the aqueous phase is extracted with dichloromethane/MeOH (7 × 100 ml, V/V 10: 1). The organic layers were collected, dried over Na<sub>2</sub>SO<sub>4</sub>, and evaporated under reduced pressure. The crude product was purified by column chromatography on silica gel flash chromatography using CH<sub>2</sub>Cl<sub>2</sub>/EtOH (50: 1 to 20: 1).

**LF1-1:** <sup>1</sup>H NMR (*d*<sub>6</sub>-DMSO, 400 MHz) δ 9.34 (s, 1H), 8.43 (d, *J* = 7.8 Hz, 1H), 8.28 (d, *J* = 9.0 Hz, 1H), 8.04 (s, 1H), 7.82 (t, *J* = 7.4 Hz, 1H), 7.74 – 7.52 (m, 3H), 4.13 (s, 3H), 3.23 (dt, *J* = 14.0, 6.6 Hz, 4H); <sup>13</sup>C NMR (DMSO, 100 MHz) δ 179.2, 178.3, 168.3, 163.6, 154.6, 146.9, 141.9, 139.7, 138.6, 137.6, 132.1, 130.6, 110.9, 67.8, 36.2,

35.3. MS (ESI)  $m/z = 263.1[M]^+$ ; HRMS(ESI) Calcd for  $C_{18}H_{15}O_2^+$  ( $[M]^+$ ): 263.1063, Found, 263.1067.

**LF1-2:**  $^1H$  NMR ( $d_6$ -DMSO, 400 MHz)  $\delta$  9.18 (s, 1H), 8.52 (d,  $J = 8.8$  Hz, 1H), 8.33 (d,  $J = 8.6$  Hz, 1H), 8.29 – 8.14 (m, 2H), 7.91 (t,  $J = 7.5$  Hz, 1H), 7.33 – 7.20 (m, 2H), 4.02 (s, 3H), 3.24 (dt,  $J = 14.0, 6.7$  Hz, 4H);  $^{13}C$  NMR (100 MHz, DMSO)  $\delta$  182.0, 178.2, 164.1, 160.6, 160.5, 147.1, 142.1, 140.3, 140.0, 139.6, 134.0, 129.0, 126.5, 124.6, 67.0, 36.7, 35.9. MS (ESI)  $m/z = 263.1[M]^+$ ; HRMS(ESI) Calcd for  $C_{18}H_{15}O_2^+$  ( $[M]^+$ ): 263.1063, Found, 263.1067.

**LF1-3:**  $^1H$  NMR ( $d_6$ -DMSO, 400 MHz)  $\delta$  9.09 (s, 1H), 8.40 (d,  $J = 8.7$  Hz, 1H), 8.17 (d,  $J = 8.9$  Hz, 1H), 7.92 (s, 1H), 7.53 (d,  $J = 8.9$  Hz, 1H), 7.28 – 7.16 (m, 2H), 4.08 (s, 3H), 3.98 (s, 3H), 3.15-3.20 (m, 4H);  $^{13}C$  NMR (100 MHz, DMSO)  $\delta$  169.5, 167.3, 167.2, 157.3, 151.1, 148.7, 131.6, 130.8, 126.6, 120.9, 119.5, 118.9, 115.9, 114.6, 101.0, 57.6, 56.8, 26.7, 25.4. MS (ESI)  $m/z = 293.1[M]^+$ ; HRMS(ESI) Calcd for  $C_{19}H_{17}O_3^+$  ( $[M]^+$ ): 293.1169, Found, 293.1172.

**LF2-1:**  $^1H$  NMR ( $d_6$ -DMSO, 400 MHz)  $\delta$  8.85 (s, 1H), 8.25 (d,  $J = 7.7$  Hz, 1H), 8.01 (d,  $J = 9.5$  Hz, 1H), 7.69 (t,  $J = 7.4$  Hz, 1H), 7.59 – 7.49 (m, 2H), 7.21 (d,  $J = 7.0$  Hz, 2H), 3.10 (s, 4H);  $^{13}C$  NMR (100 MHz, DMSO)  $\delta$  163.5, 140.1, 137.4, 134.2, 133.2, 131.4, 129.4, 125.2, 107.8, 31.3, 29.8. MS (ESI)  $m/z = 249.1[M]^+$ ; HRMS(ESI) Calcd for  $C_{17}H_{13}O_2^+$  ( $[M]^+$ ): 249.0907, Found, 249.0910.

**LF2-2:**  $^1H$  NMR ( $d_6$ -DMSO, 400 MHz)  $\delta$  7.83 (dd,  $J = 31.6, 9.1$  Hz, 1H), 7.58 (d,  $J = 7.7$  Hz, 1H), 7.38 – 7.28 (m, 1H), 7.21 – 7.13 (m, 1H), 7.10 – 6.91 (m, 1H), 6.86 – 6.63 (m, 2H), 6.31 – 6.07 (m, 1H), 2.88 – 2.70 (m, 4H);  $^{13}C$  NMR (100 MHz, DMSO)  $\delta$  162.3, 161.3, 158.4, 146.1, 132.9, 131.8, 131.3, 131.2, 130.4, 128.9, 115.8, 114.9, 114.2, 105.2, 101.5, 28.7, 27.4. MS (ESI)  $m/z = 249.1[M]^+$ ; HRMS(ESI) Calcd for  $C_{17}H_{13}O_2^+$  ( $[M]^+$ ): 249.0907, Found, 249.0910.

**LF2-3:**  $^1H$  NMR ( $d_6$ -DMSO, 400 MHz)  $\delta$  9.04 (s, 1H), 8.39 (d,  $J = 8.3$  Hz, 1H), 8.12 (d,  $J = 8.7$  Hz, 1H), 7.51 (s, 1H), 7.38 (dd,  $J = 8.9, 1.3$  Hz, 1H), 7.18 (d,  $J = 8.5$  Hz, 2H), 3.96 (s, 3H), 3.18 – 3.12 (m, 4H);  $^{13}C$  NMR (100 MHz, DMSO)  $\delta$  168.5, 167.4,



sulfuric acid, 90°C, 5 h; (b) 70% HClO<sub>4</sub>, room temperature, 10 min.

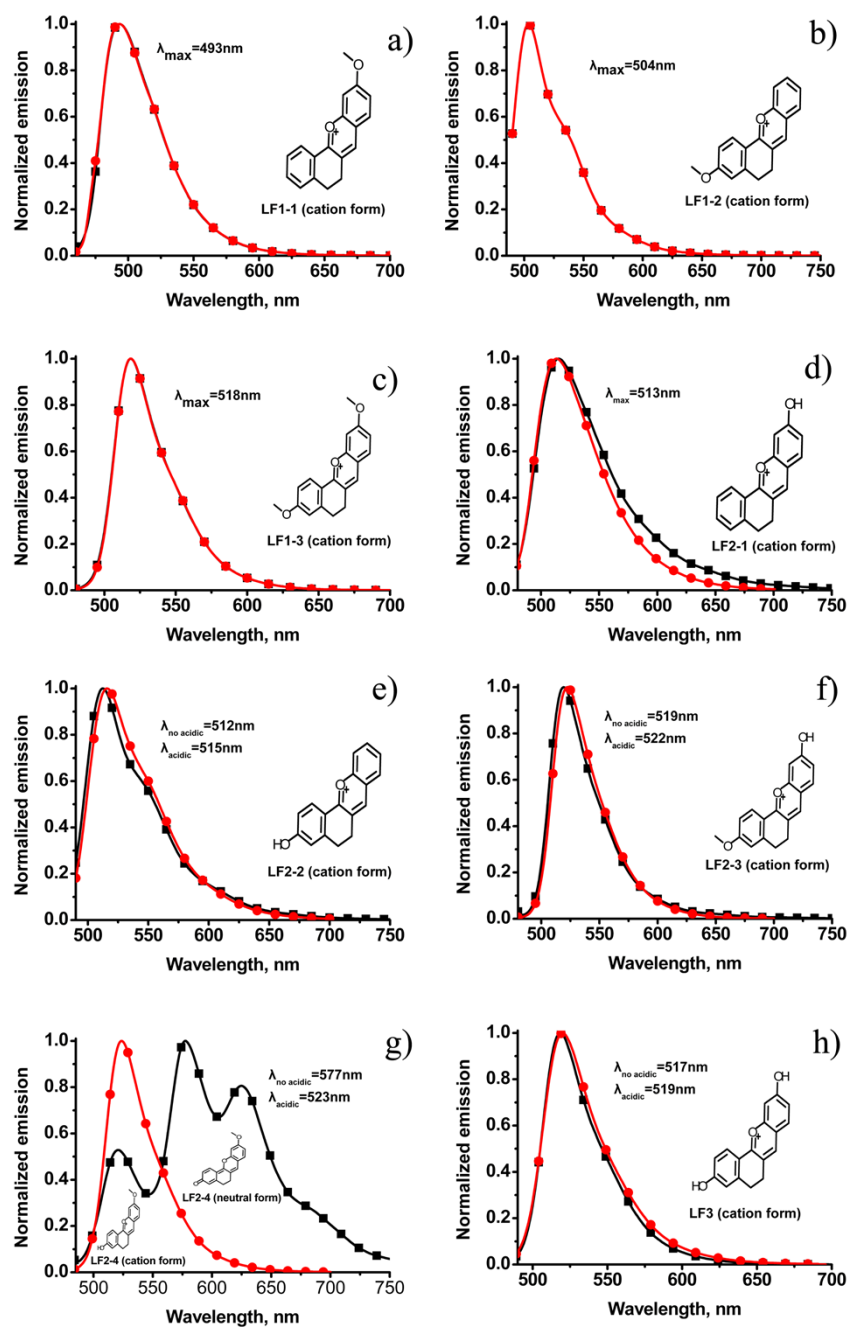
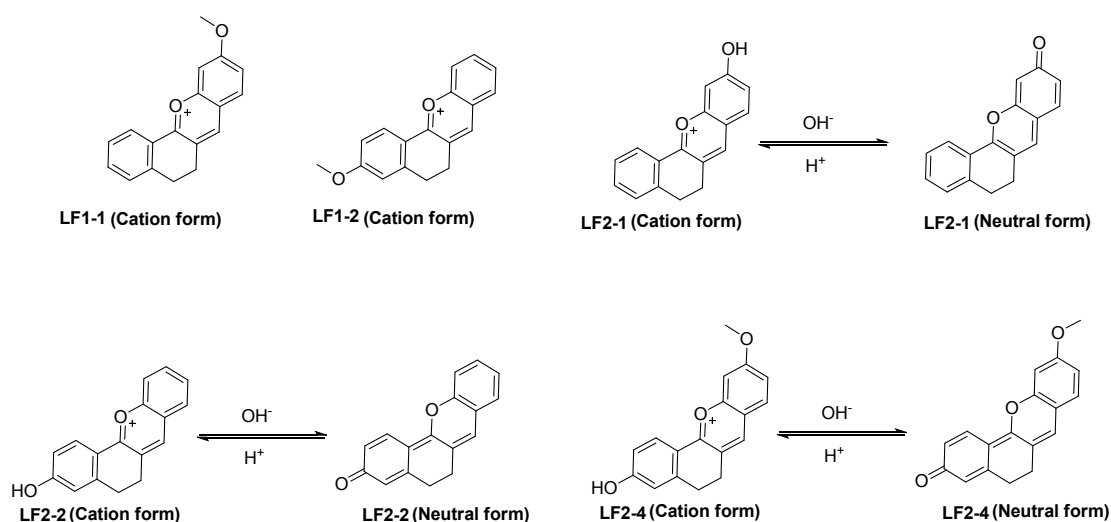


**Figure S1.** The normalized fluorescence emission spectra of compounds **LF1-1(a)**, **LF1-2(b)**, **LF1-3(c)**, **LF2-1(d)**, **LF2-2(e)**, **LF2-3(f)**, **LF2-4(g)** and **LF3(h)** (5  $\mu\text{M}$ ) in  $\text{CH}_2\text{Cl}_2$  (■) and  $\text{CH}_2\text{Cl}_2$  containing 1% HCl (●).



**Scheme S2.** Equilibrium forms of LF1-1, LF1-2, LF2-1, LF2-2 and LF2-3.

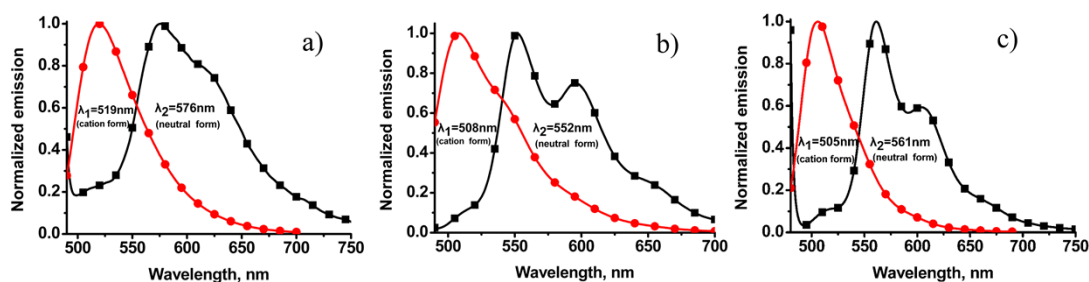


**Figure S2.** The normalized fluorescence emission spectra of compounds LF2-1 (a), LF2-2 (b) and LF2-4 (c) (5  $\mu$ M) in PBS at different pH values: pH = 1 (■), pH = 7.5 (●).

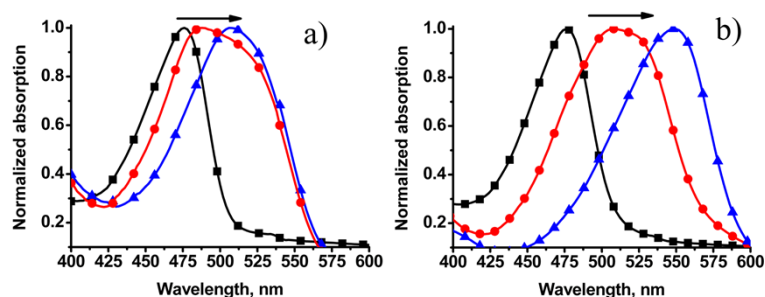


**Figure S3.** The normalized absorption spectra of compounds LF2-3 (a) pH = 1 (■) and pH = 7.5 (▲); LF3 (b) at different pH values: pH = 1 (■), pH = 5.5 (●) and pH = 7.5 (▲).



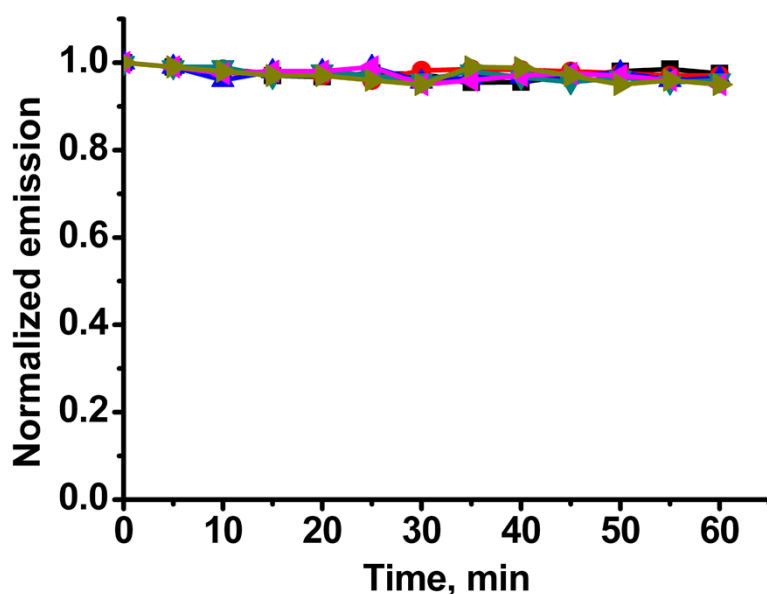


**Figure S4.** Normalized emission of LF2-1(■), LF2-2(▲), LF2-3(◄), LF2-4(◄) and LF3 (●) as the function of irradiation time in PBS.

**Table S1.** Calculated absorption and emission wavelengths and oscillator strengths of LF dyes. Emission wavelength and oscillator strength were obtained from Gaussian 09 programs using the B3LYP exchange functional, together with 6-31+G(d) basis sets.

compound	absorption wavelength (nm)	Oscillator strength ( <i>f</i> )	Emission wavelength (nm)	Oscillator strength ( <i>f</i> )
<b>LF2-1(cation)</b>	438	0.612	474	0.541
<b>LF2-1(neutral)</b>	481	0.514	592	0.346
<b>LF2-2(cation)</b>	430	0.872	463	0.784
<b>LF2-2(neutral)</b>	453	0.928	538	0.729
<b>LF2-3(cation)</b>	445	0.866	475	0.825
<b>LF2-3(neutral)</b>	488	0.669	574	0.475
<b>LF2-4(cation)</b>	452	0.889	474	0.868
<b>LF2-4(neutral)</b>	463	1.070	531	0.898
<b>LF3(cation)</b>	439	0.828	461	0.822
<b>LF3(neutral)</b>	485	0.619	531	0.829
<b>LF3(anionic)</b>	515	0.944	575	0.434

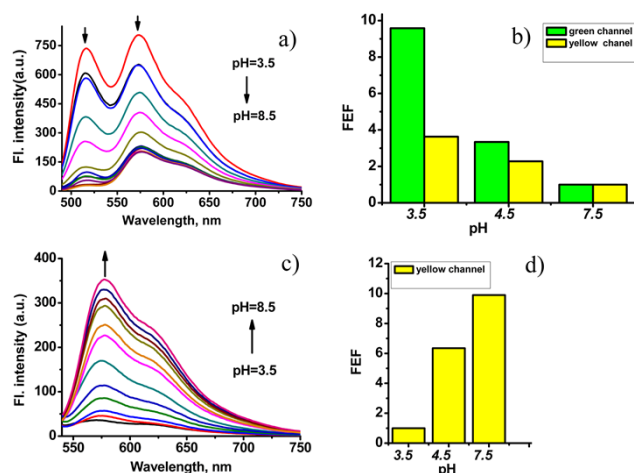


**Figure S5.** a) pH-dependence of the fluorescence intensity of **LF2-3** ( $5 \mu\text{M}$ ) with the arrow indicating the change of the fluorescence intensities with pH increase from 3.5 to 8.5, excitation at 470 nm; b) the fluorescence enhanced factor (FEF) of **LF2-3** with pH increase from 3.5 to 8.5 in green, yellow emission channels, excitation at 470 nm; c) pH-dependence of the fluorescence intensity of **LF2-3** ( $5 \mu\text{M}$ ) with the arrow indicating the change of the fluorescence intensities with pH increase from 3.5 to 8.5, excitation at 520 nm; d) the fluorescence enhanced factor (FEF) of **LF2-3** with pH increase from 3.5 to 8.5 in green, yellow emission channels, excitation at 520 nm. Spectra were obtained with in 25 mM PBS (containing 1 %  $\text{CH}_3\text{CH}_2\text{OH}$  as a co-solvent). The green and yellow emission channels are centered at 514 and 576 nm, respectively.

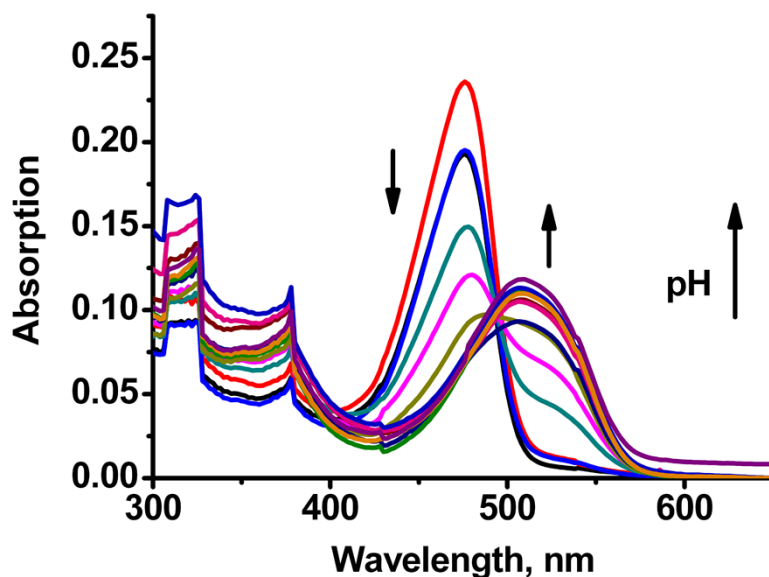


**Figure S6.** pH-dependence of the absorption intensity of **LF2-3** ( $5 \mu\text{M}$ ) with the arrow indicating the change of the fluorescence intensities with pH increase from 3.5 to 8.5. Spectra were obtained in 25 mM PBS (containing 1 %  $\text{CH}_3\text{CH}_2\text{OH}$  as a co-solvent).

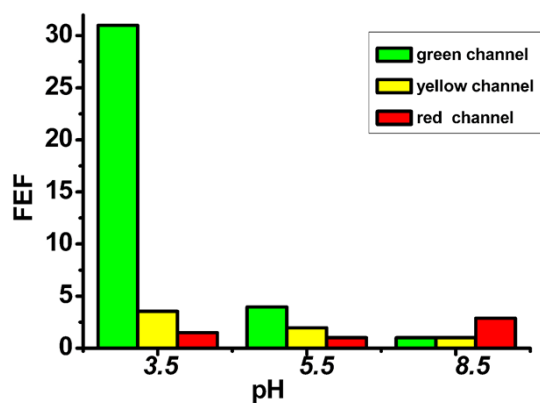


**Figure S7.** The fluorescence enhanced factor (FEF) of LF3 with pH increase from 3.5 to 8.5 in green, yellow and red emission channels, excitation at 470 nm; Spectra were obtained in 25 mM PBS (containing 1 % CH<sub>3</sub>CH<sub>2</sub>OH as a co-solvent). The green, yellow, and red emission channels centered at 515, 566, and 593 nm, respectively.

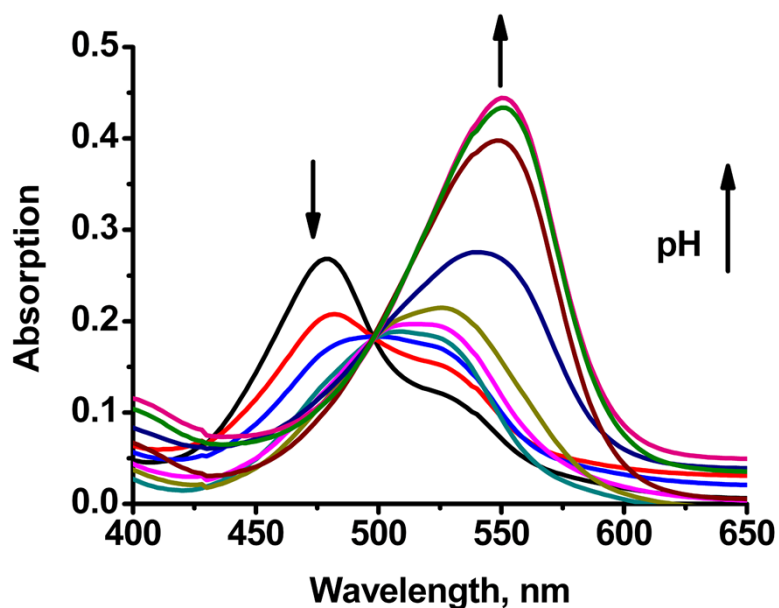


**Figure S8.** pH-dependence of the absorption intensity of LF3 (5 μM) with the arrow indicating the change of the fluorescence intensities with pH increase from 3.5 to 8.5. Spectra are obtained in 25 mM PBS (containing 1 % CH<sub>3</sub>CH<sub>2</sub>OH as a co-solvent).

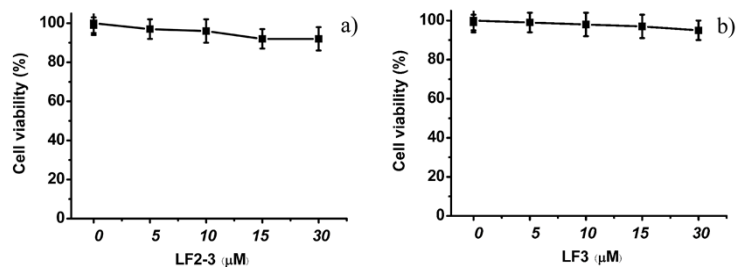


**Figure S9.** Cytotoxicity of the **LF2-3** and **LF3** on HeLa cells determined by MTT.

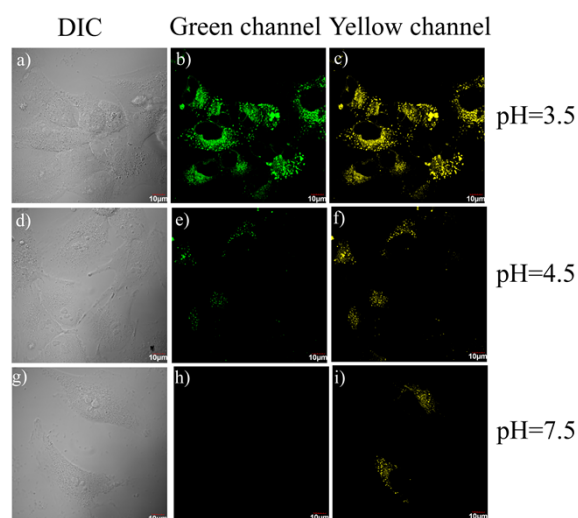


**Figure S10.** Brightfield and fluorescence images of HeLa cells stained with **LF2-3** at PBS of different pH values: (a-c) Brightfield and fluorescence images of the cells incubated with **LF2-3** (5 μM) at pH = 3.5: (a) Brightfield image; (b) Fluorescence image from the green channel; (c) Fluorescence image from the yellow channel; (d-f) Brightfield and fluorescence images of the cells incubated with **LF2-3** (5 μM) at pH = 4.5: (d) Brightfield image; (e) Fluorescence image from the green channel; (f) Fluorescence image from the yellow channel; (g-i) Brightfield and fluorescence images of the cells incubated with **LF2-3** (5 μM) at pH = 7.5: (g) Brightfield image; (h) Fluorescence image from the green channel; (i) Fluorescence image from the yellow channel. The green and yellow channels are corresponding to the emission windows of 490-530 nm and 540-580 nm, respectively. Excitation at 488 nm. Scale bar = 10 μm.

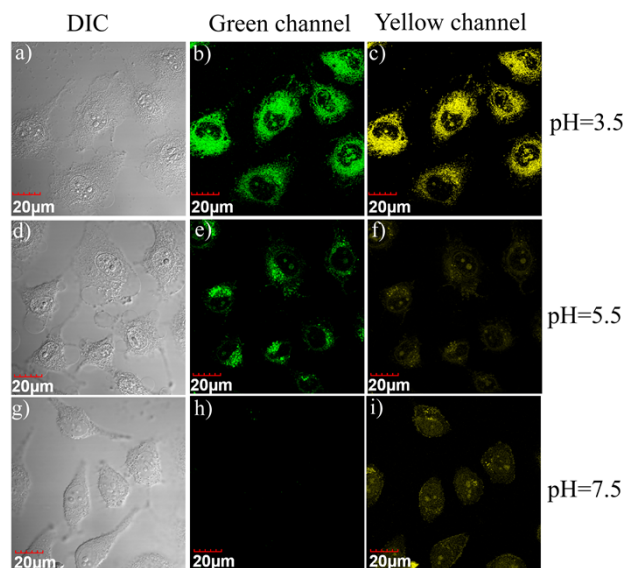


**Figure S11.** Brightfield and fluorescence images of HeLa cells stained with **LF2-3** at Britton-Robinson buffers of different pH values: (a-c) Brightfield and fluorescence images of the cells incubated with **LF2-3** (5  $\mu\text{M}$ ) at pH = 3.5: (a) Brightfield image; (b) Fluorescence image from the green channel; (c) Fluorescence image from the yellow channel; (d-f) Brightfield and fluorescence images of the cells incubated with **LF2-3** (5  $\mu\text{M}$ ) at pH = 4.5: (d) Brightfield image; (e) Fluorescence image from the green channel; (f) Fluorescence image from the yellow channel; (g-i) Brightfield and fluorescence images of the cells incubated with **LF2-3** (5  $\mu\text{M}$ ) at pH = 7.5: (g) Brightfield image; (h) Fluorescence image from the green channel; (i) Fluorescence image from the yellow channel. The green and yellow channels are corresponding to the emission windows of 490-530 nm and 540-580 nm, respectively. Excitation at 488 nm. Scale bar = 10  $\mu\text{m}$ .

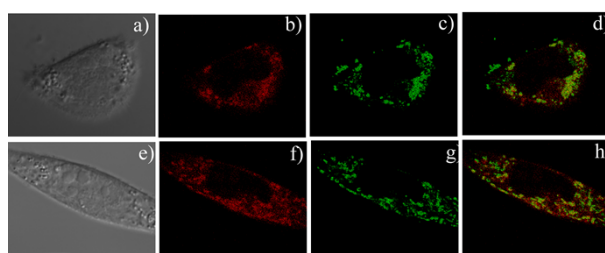


**Figure S12.** Confocal fluorescence images of **LF-3** (5  $\mu\text{M}$ ) incubated with 1  $\mu\text{M}$  LysoTracker green (a-d) or 1  $\mu\text{M}$  Mitotracker green FM (e-h) in living HeLa cells with PBS (pH=7.4). Images were acquired using (b, f) 488 nm excitation and emission channel of 580–640 nm (red), (c: LysoTracker green; g: Mitotracker green FM) 488 nm excitation and emission channel of 500–550 nm (green); (d, g) merged images of red and green channels; Scale bar = 10  $\mu\text{m}$ .

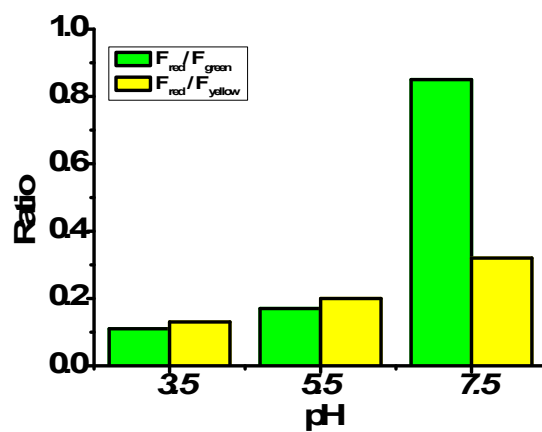


**Figure S13.** Average  $F_{red}/F_{green}$  and  $F_{red}/F_{yellow}$  intensity ratios of the HeLa cells stained with LF3 at different pH values.

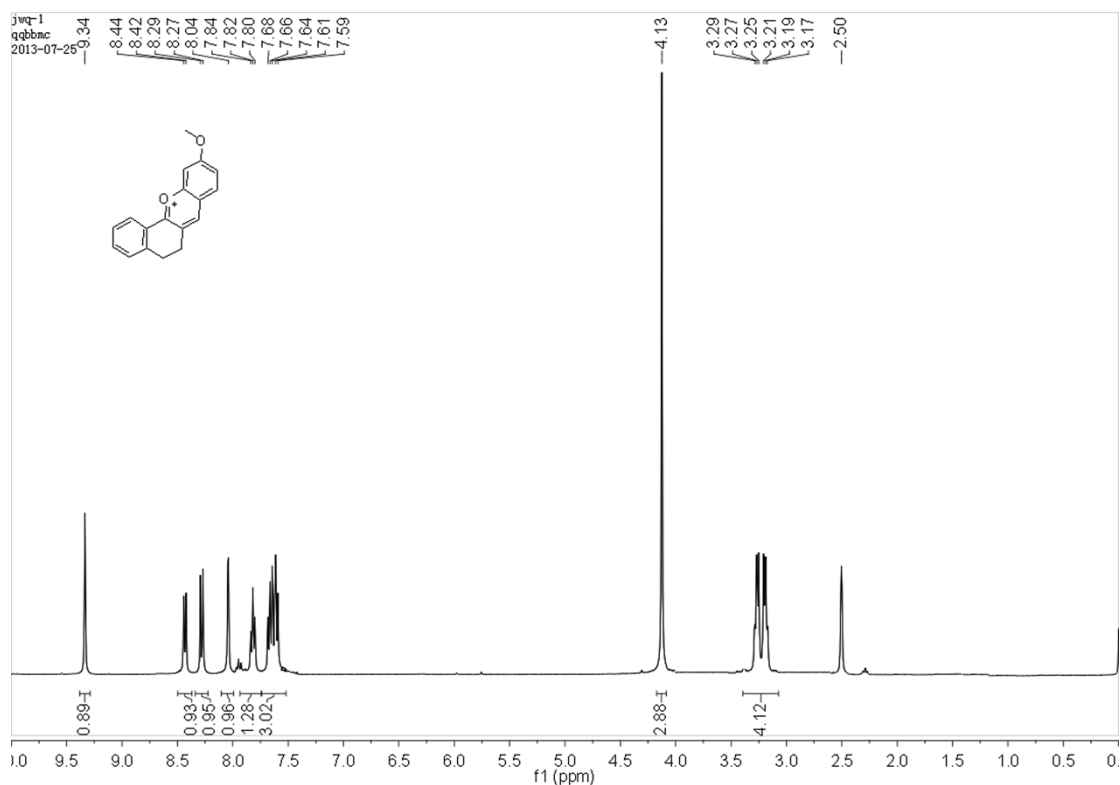


**Figure S14.**  $^1\text{H}$  NMR spectrum of LF1-1 ( $d^6$ -DMSO).

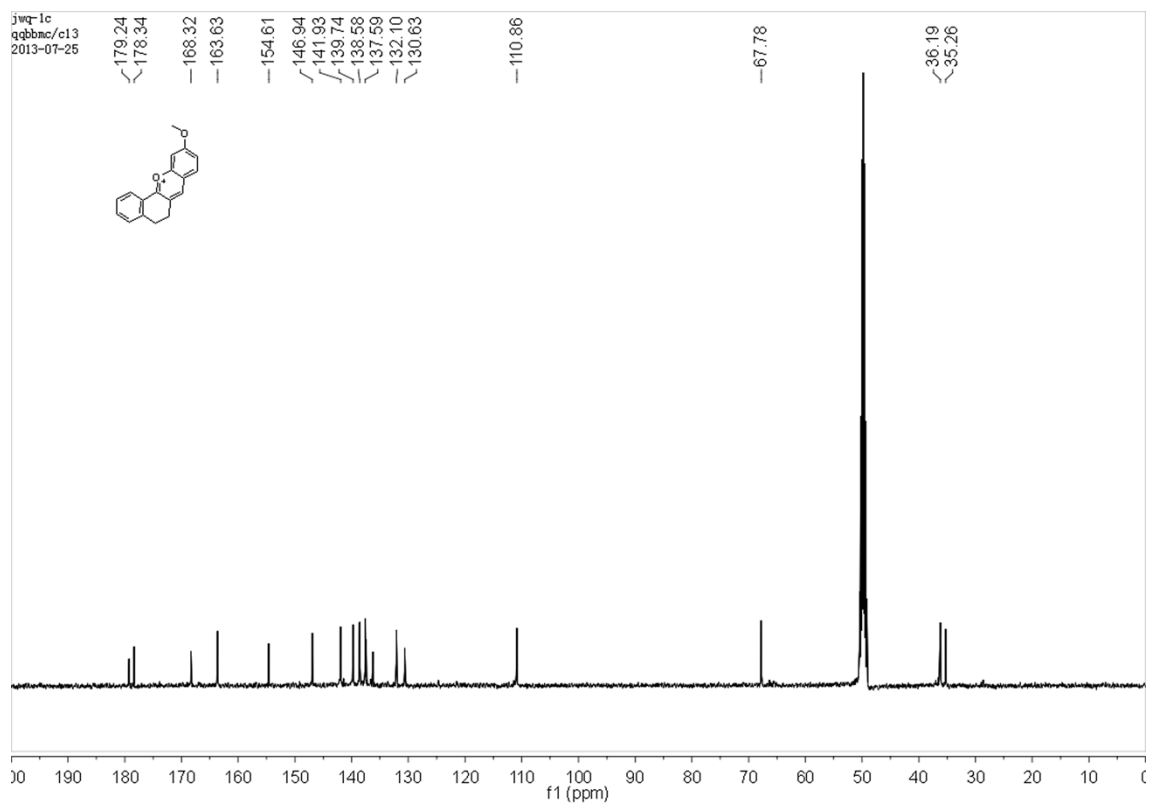


**Figure S15.**  $^{13}\text{C}$  NMR spectrum of LF1-1 ( $d^6$ -DMSO).

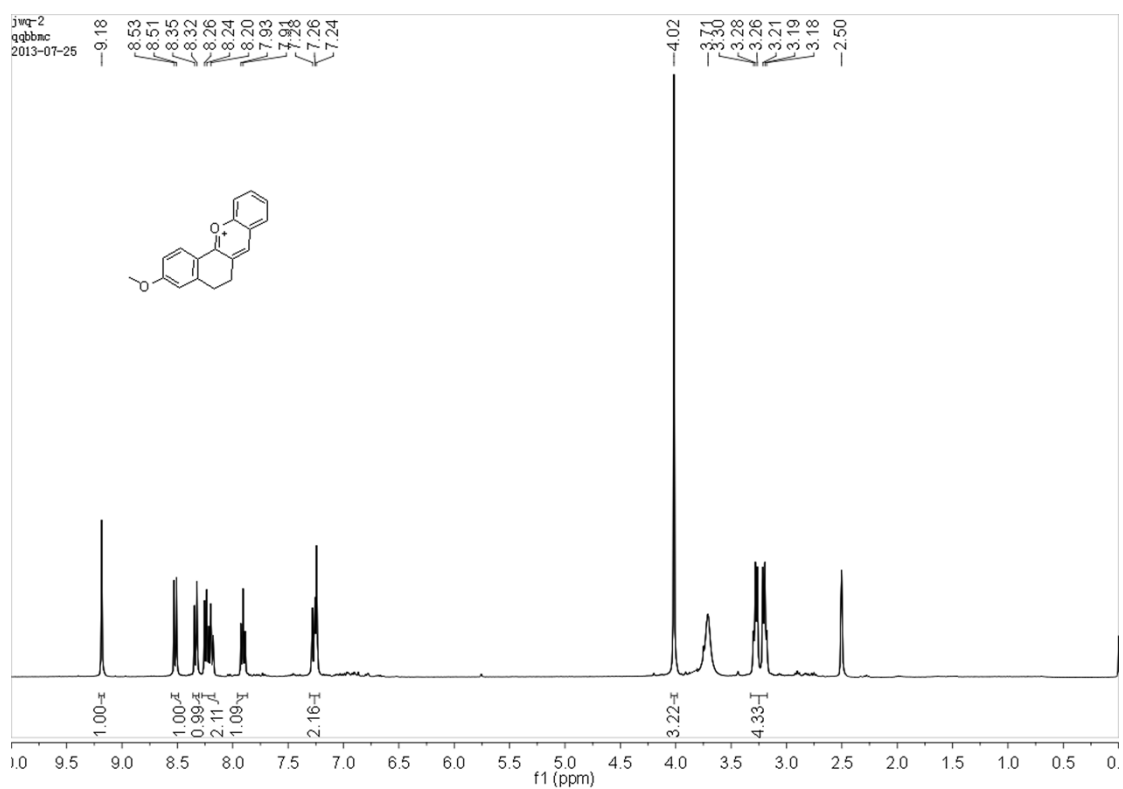


**Figure S16.**  $^1\text{H}$  NMR spectrum of LF1-2 ( $d^6$ -DMSO).

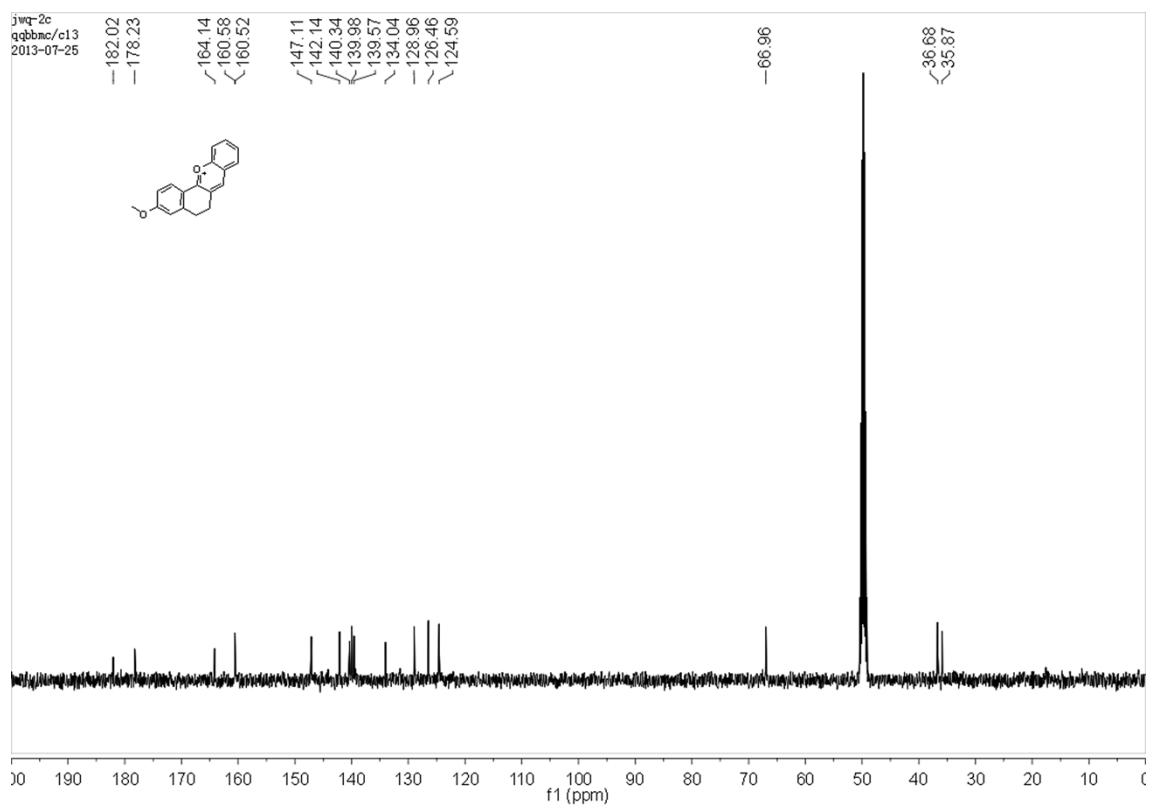


**Figure S17.**  $^{13}\text{C}$  NMR spectrum of LF1-2 ( $d^6$ -DMSO).

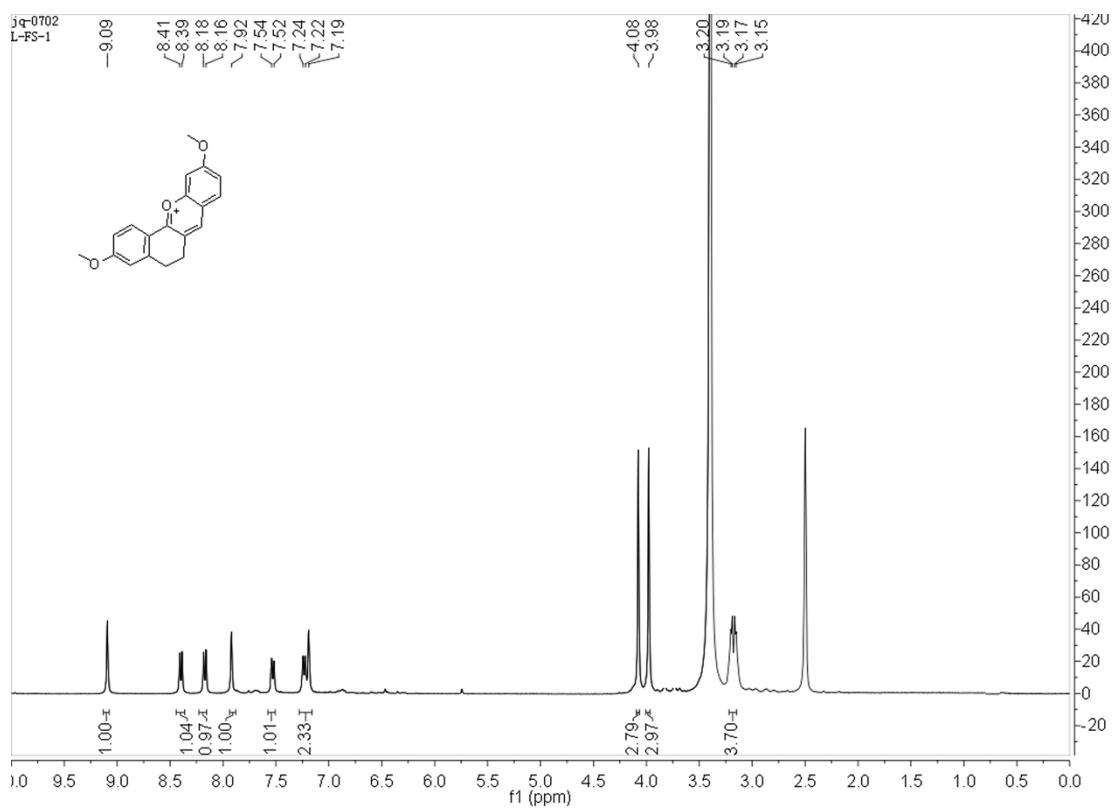




**Figure S18.**  $^1\text{H}$  NMR spectrum of LF1-3 ( $d^6$ -DMSO).

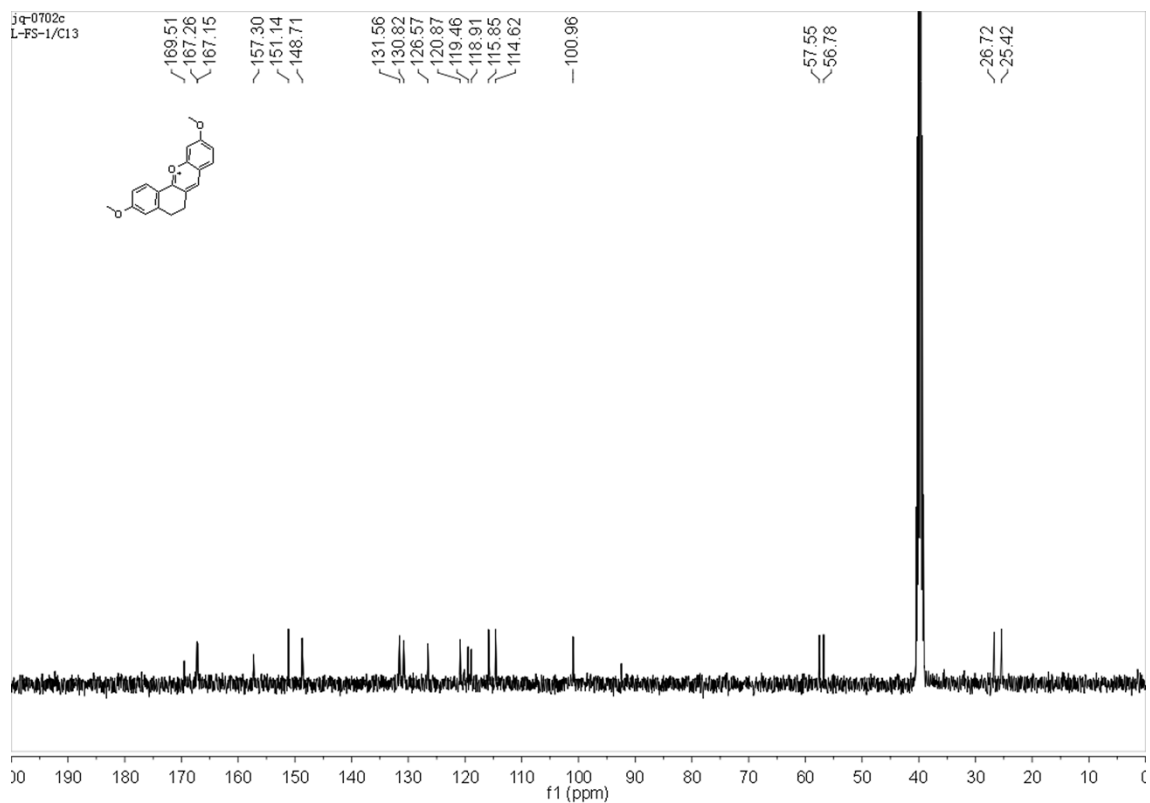


**Figure S19.**  $^{13}\text{C}$  NMR spectrum of LF1-3 ( $d^6$ -DMSO).

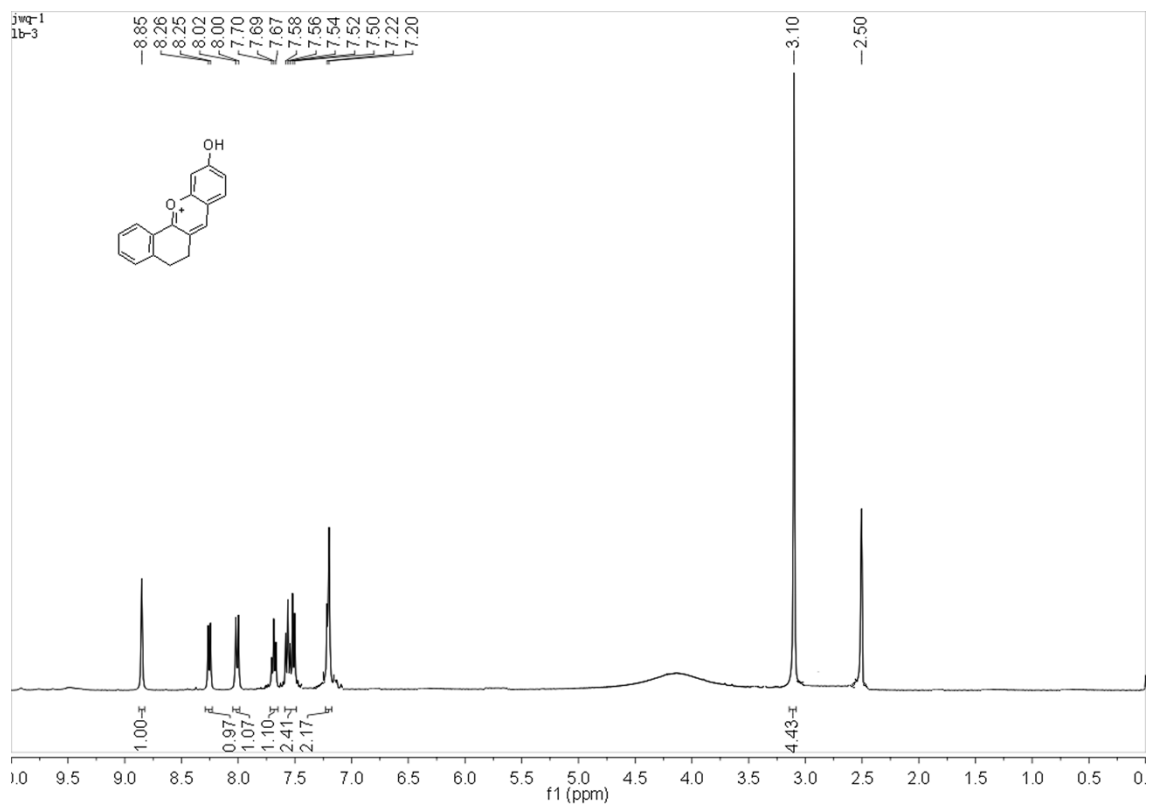


**Figure S20.**  $^1\text{H}$  NMR spectrum of LF2-1 ( $d^6$ -DMSO).

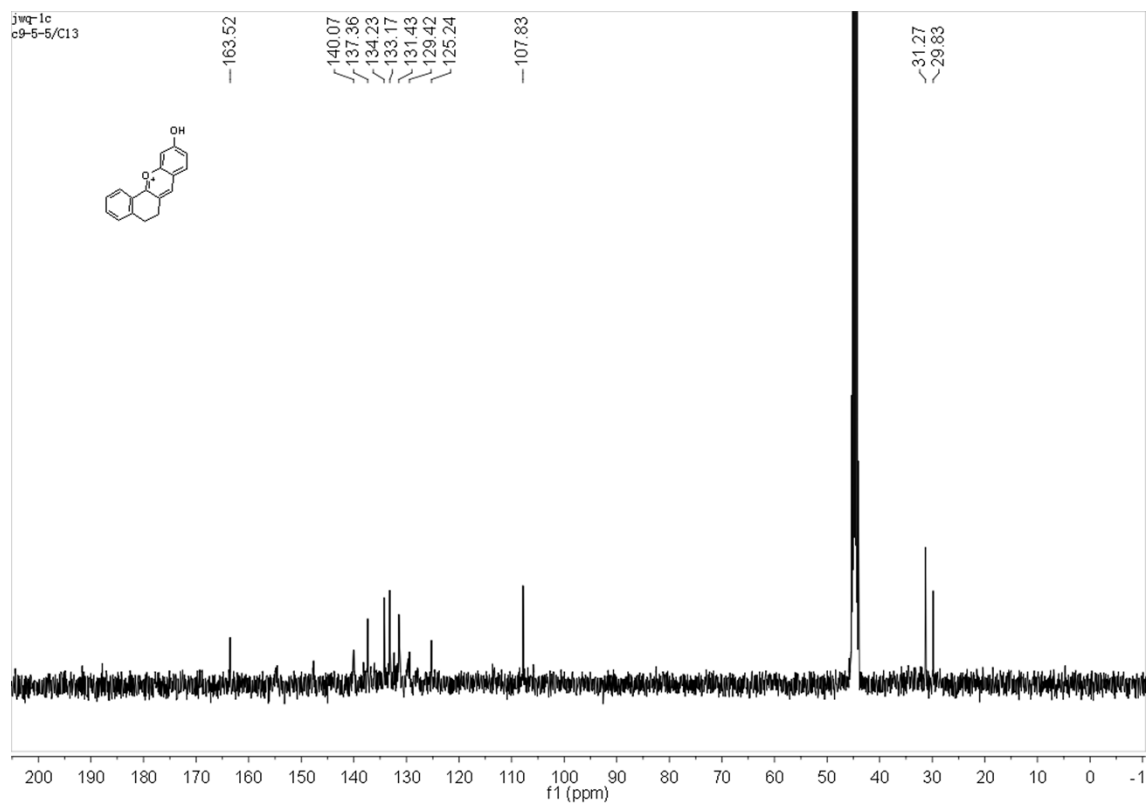


**Figure S21.**  $^{13}\text{C}$  NMR spectrum of LF2-1 ( $d^6$ -DMSO).

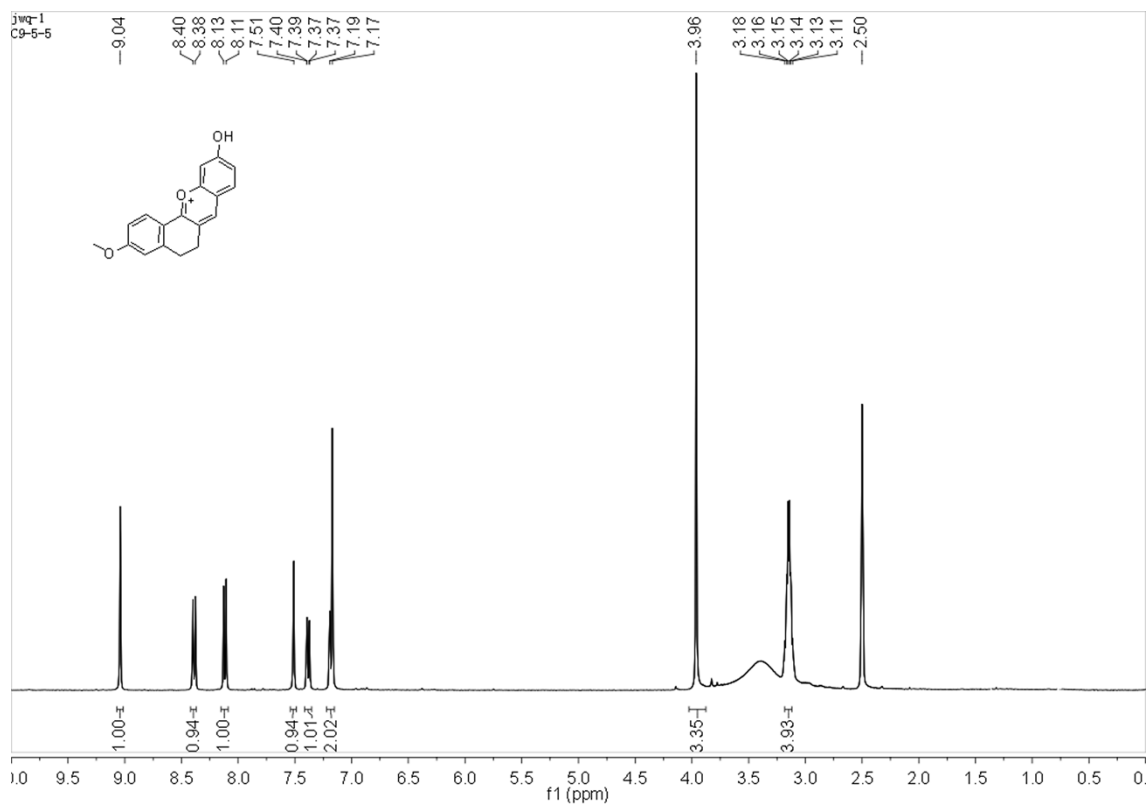


**Figure S22.**  $^1\text{H}$  NMR spectrum of LF2-3 ( $d^6$ -DMSO).

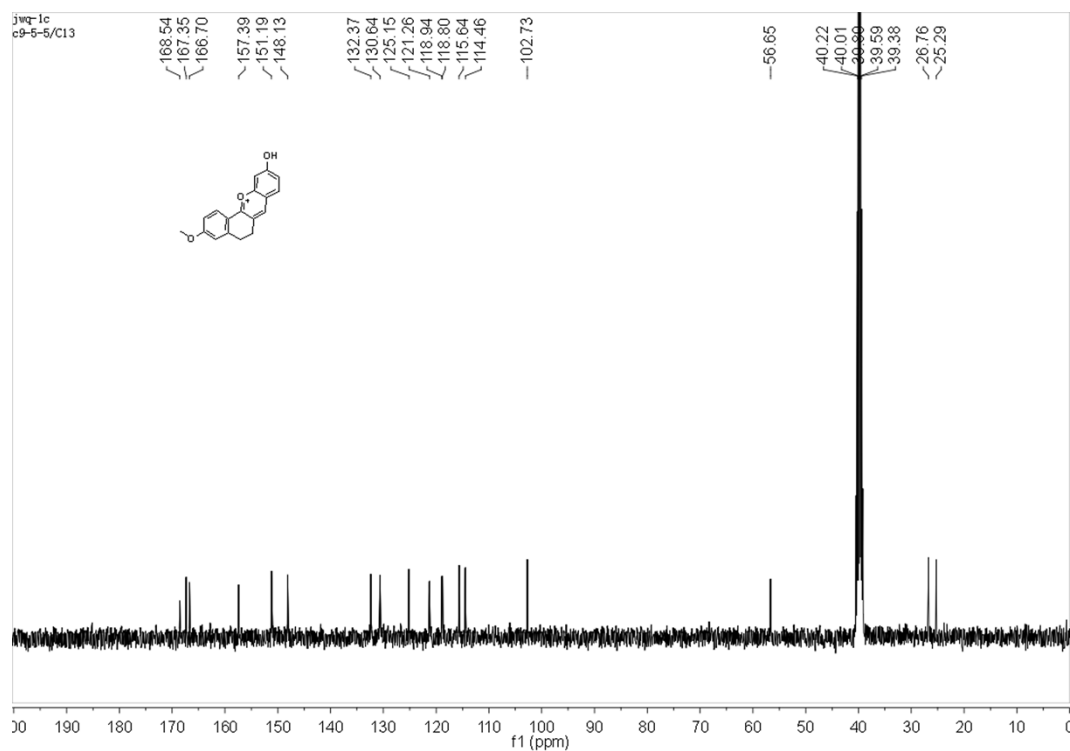


**Figure S23.**  $^{13}\text{C}$  NMR spectrum of LF2-3 ( $d^6$ -DMSO).